



# Sedimentation equilibrium analysis of recombinant mouse FcRn with murine IgG1

Peter Schuck<sup>a</sup>, Caius G. Radu<sup>b</sup>, E. Sally Ward<sup>b,\*</sup>

<sup>a</sup>*Molecular Interactions Resource ORS, Bioengineering and Physical Science Program, National Institutes of Health, 13 South Drive, Bethesda, MD 20892-5766, USA*

<sup>b</sup>*Center for Immunology and Cancer Immunobiology Center, University of Texas Southwestern Medical Center, 5323 Harry Hines Blvd, Dallas, TX 75235-8576, USA*

Received 5 May 1999; accepted 8 June 1999

## Abstract

The interaction of mouse IgG1 or IgG1-derived Fc fragment with recombinant, insect cell expressed mouse FcRn has been analyzed using sedimentation equilibrium. This results in a model for the interaction in which the two binding sites for FcRn on Fc or IgG1 have significantly different affinities with macroscopic binding constants of <130 nM and 6 μM. This data indicates the formation of an asymmetric FcRn:Fc (or IgG1):FcRn complex which is consistent with earlier suggestions that for this form of recombinant FcRn, binding to IgG1 or Fc does not result in a symmetric 2:1 complex in which both binding sites are equivalent. © 2000 Elsevier Science Ltd. All rights reserved.

*Keywords:* Neonatal Fc receptor; Sedimentation equilibrium; Murine IgG1

## 1. Introduction

The MHC class I related receptor, FcRn (Simister and Mostov, 1989), has been shown to be involved in both the transfer of gammaglobulins (IgGs) from mother to young (Israel et al., 1995; Roberts et al., 1990; Rodewald et al., 1983; Simister and Rees, 1985) and the regulation of serum IgG levels (Ghetie et al., 1996; Israel et al., 1996; Junghans and Anderson, 1996). The available data indicate that it carries out these functions by acting as a transcytotic and/or recycling receptor whereby it binds and transports IgGs in intact form within and across cells (reviewed in Ghetie and Ward, 1997; Junghans, 1997). This receptor binds to the Fc region of IgG, and amino acids at the CH2–CH3 domain interface play a central role in the interaction (Burmeister et al., 1994; Kim et al., 1994a;

Medesan et al., 1997; Raghavan et al., 1994). The interaction is highly pH dependent with high affinity binding occurring at pH 6.0–6.5 and undetectable binding at a pH above 7.0 (Popov et al., 1996; Raghavan et al., 1994; Rodewald and Kraehenbuhl, 1984; Simister and Rees, 1985). This strict pH dependence is most likely due to the involvement of histidines of the Fc region (Kim et al., 1994a; Raghavan et al., 1994). Evidence for an indirect role for FcRn histidines in mediating a pH dependent interaction has also been presented (Raghavan et al., 1994, 1995a).

The symmetry of the IgG molecule suggests that the interaction of FcRn with IgG or Fc may occur with a stoichiometry of two FcRn molecules to one Fc or IgG molecule. Functional studies in mice using an ‘Fc-hybrid’ which has only one functional FcRn binding site per molecule indicated that two functional sites per IgG (or Fc) are needed for FcRn-mediated activity (Kim et al., 1994b). Consistent with this, in co-crystals of rat FcRn and Fc a network of two types of complexes are seen (Burmeister et al., 1994); one of these types of complexes comprises ‘standing up’ complexes

\* Corresponding author. Tel.: +1-214-648-1260; fax: +1-214-648-1259.

E-mail address: sally@skylab.swmed.edu (E.S. Ward).

in which two FcRn molecules bind to one Fc whereas the other type of complex is an asymmetric 'lying down' complex in which an FcRn dimer interacts with one Fc. However, solution studies of FcRn and IgG/Fc have resulted in conflicting results for the FcRn:IgG/Fc stoichiometry, with data in support of the formation of 2:1 (Huber et al., 1993) or 1:1 (Popov et al., 1996) complexes being reported. These differences may be due to the differences in the sources of recombinant protein (expressed in insect or mammalian cells) and/or species of FcRn (mouse or rat) used in the two studies.

The 1:1 stoichiometry obtained by our *in vitro* studies of insect cell expressed FcRn (mouse derived) using gel filtration and other methods (Popov et al., 1996) is inconsistent with the need for two functional sites per Fc for activity in FcRn-mediated trafficking *in vivo* (Kim et al., 1994b). To reconcile the apparent discrepancies between the 1:1 complex formed *in vitro* and our functional data for the Fc-hybrid, we therefore proposed an asymmetric model for the Fc:FcRn interaction (Ghetie and Ward, 1997). In this model we suggested that the Fc molecule is asymmetric with respect to FcRn binding, and when one site is occupied, the affinity of the other site decreases. This is also consistent with a structural model for Fc:FcRn complexation proposed recently in which the CH2 domain reorientates itself following interaction with FcRn (Weng et al., 1998) and earlier suggestions that Fc may be distorted by FcRn binding (Burmeister et al., 1994). In the current study, the affinity and stoichiometry of interaction of recombinant, insect cell expressed mouse FcRn with mouse IgG1 or Fc (IgG1-derived) has been analyzed using sedimentation equilibrium experiments. The results provide support for the concept that the FcRn interaction sites on IgG/Fc have significantly different affinities, and for this particular interaction involving mouse IgG1 (or Fc) and recombinant FcRn the macroscopic affinity constants differ by about 50 fold.

## 2. Materials and methods

### 2.1. Antibodies

Mouse IgG1 was obtained from the RFB4 hybridoma as described previously (Kim et al., 1994a). The mouse IgG1-derived Fc fragment was prepared by papain digestion at pH 6.0 and purified using protein A-Sepharose (Kim et al., 1994a).

### 2.2. Mouse FcRn

Mouse FcRn was expressed and purified from baculovirus infected High-5 cells (Popov et al., 1996). Prior

to use in sedimentation equilibrium experiments, FcRn was analyzed by FPLC using a Superdex 200 column (Pharmacia) and a Bio-Rad BioLogic workstation.

### 2.3. Analytical ultracentrifugation

Sedimentation equilibrium experiments were performed using a Beckman Optima XL-A with an An60-Ti 8-hole rotor and absorbance optical system. Double sector charcoal-filled epon centerpieces were filled with between 130 and 180  $\mu$ l of protein at concentrations in the range between approximately 0.05 and 5  $\mu$ M in phosphate buffered saline, pH 6.0. Sedimentation equilibrium was attained at a rotor temperature of 4°C at several different rotor speeds between 12,000 and 18,000 rpm. Absorbance distributions were recorded at wavelengths of 230, 250, 280, 300 and 305 nm. These wavelengths were chosen according to the protein concentration to allow the reliable observation of a large section of the sedimentation profile, i.e. at absorbance values with optimal signal-to-noise ratios within the linear range of the optics (below approximately 1.3 OD). The extinction coefficients at a wavelength of 280 nm were calculated from the amino acid composition using the program Sednterp (Laue et al., 1992), and the extinction coefficients at all other wavelengths were determined spectrophotometrically by measuring the absorbance ratio at different wavelengths. Alternatively, the absorbance ratios were determined from scanning the concentration gradients in sedimentation equilibrium at different wavelengths followed by least-squares calculation of the scaling factor between the absorbance profiles.

Data analysis was performed according to standard procedures (reviewed in Rivas et al., 1999). Global analysis was applied to several data sets obtained at different loading concentrations, molar ratios of interacting proteins and/or rotor speeds. The absence of thermodynamic non-idealities was observed in the sedimentation profiles of the individual proteins over the concentration range used in the binding studies, and the absence of pressure effects on the affinity constants of the interaction was assumed. For the analysis of the interactions of FcRn with Fc, each sedimentation profile was modeled by a superposition of the well-known equilibrium distributions of thermodynamically ideal components (Rivas et al., 1999). A detailed description of the model for the interaction of FcRn with Fc follows; an analogous treatment was used for the interaction of FcRn and IgG1. The species considered are the free FcRn and the free Fc, with radial absorbance distributions  $A_{\text{FcRn}}(r)$  and  $A_{\text{Fc}}(r)$ , respectively, plus terms for reversible complexes formed by FcRn and Fc,  $A_{1:1}(r)$  and  $A_{2:1}(r)$  for the 1:1 complex and the 2:1 complex, respectively:

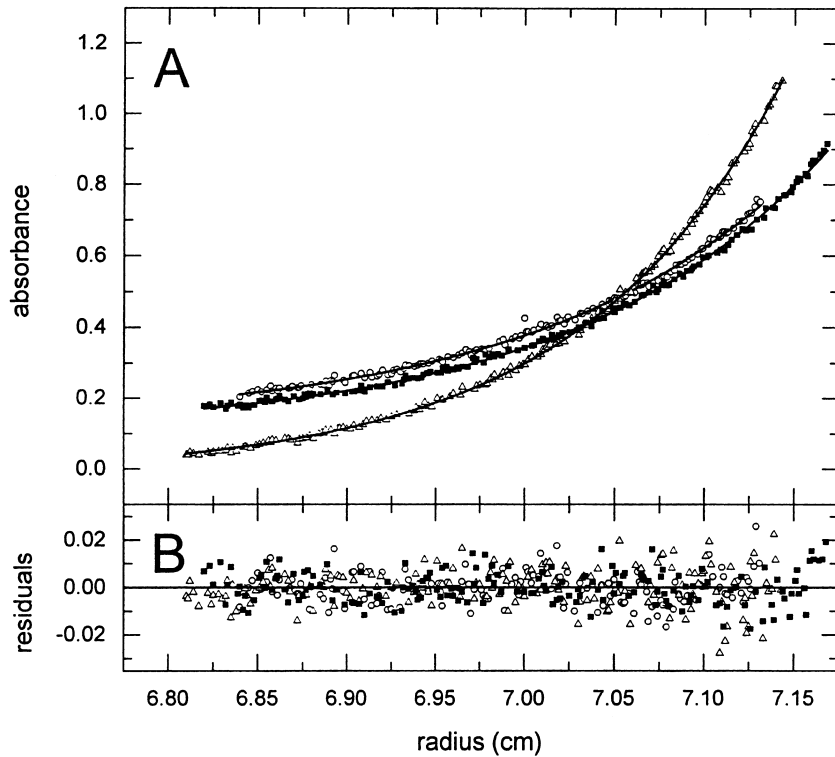


Fig. 1. A: Absorbance profiles of FcRn (circles), Fc (squares), and IgG (triangles) in sedimentation equilibrium at rotor speeds of 12,000 rpm (FcRn and Fc) and 8000 rpm (IgG), respectively. The sedimentation profiles were scanned at a wavelength of 250 nm. Best-fit distributions (solid lines) are based on the theoretical distribution of a single ideal macromolecular component in sedimentation equilibrium, with buoyant molar masses of 13,500 Da for FcRn, 14,500 Da for Fc and 40,660 kDa for the IgG. B: Residuals of the fits.

$$A(r) = A_{FcRn}(r) + A_{Fc}(r) + A_{1:1}(r) + A_{2:1}(r) + \delta \quad (1)$$

with

$$A_{FcRn}(r) = c_{FcRn} \epsilon_{\lambda, FcRn} \exp[M_{FcRn}^* \sigma (r^2 - r_0^2)]$$

$$A_{Fc}(r) = c_{Fc} \epsilon_{\lambda, Fc} \exp[M_{Fc}^* \sigma (r^2 - r_0^2)]$$

$$A_{1:1}(r) = c_{Fc} c_{FcRn} K_A^{(1:1)} (\epsilon_{\lambda, Fc} + \epsilon_{\lambda, FcRn}) \exp[(M_{Fc}^* + M_{FcRn}^*) \sigma (r^2 - r_0^2)]$$

$$A_{2:1}(r) = c_{Fc} (c_{FcRn})^2 K_A^{(1:1)} K_A^{(2:1)} (\epsilon_{\lambda, Fc} + 2\epsilon_{\lambda, FcRn}) \times \exp[(M_{Fc}^* + 2M_{FcRn}^*) \sigma (r^2 - r_0^2)]. \quad (2)$$

In these equations,  $c_{FcRn}$  and  $c_{Fc}$  denote the concentrations of free Fc and FcRn at a reference radius  $r_0$ ,  $\epsilon_{\lambda, Fc}$  and  $\epsilon_{\lambda, FcRn}$  denote their respective extinction coefficient at wavelength  $\lambda$ ,  $M^*$  denotes the buoyant molar mass  $M(1 - \bar{v}\rho)$ ,  $\sigma$  abbreviates the factor  $\omega^2/2RT$  (with the gas constant  $R$  and absolute temperature  $T$ ), and  $\delta$  denotes a small baseline offset. Since in sedimentation equilibrium analyses of interacting, ideal components in the absence of pressure effects the species

described by Eq. (2) are also in chemical equilibrium and obey the mass action law (Rivas et al., 1999),  $K_{A(1:1)}$  is the macroscopic association constant of the formation of a 1:1 complex, and  $K_{A(2:1)}$  is the macroscopic association constant for the addition of a second FcRn molecule to the 1:1 complex to form the 2:1 complex. The free energy of binding was calculated according to  $\Delta G = RT \log(K_A)$ , where  $K_A$  denotes the microscopic binding constant (which is equal to the macroscopic binding constants in the case of non-equivalent sites, and related to the macroscopic binding constants by a statistical factor of 2 (or  $\frac{1}{2}$ , respectively) in the case of two equivalent binding sites per molecule).

For global fitting with Eqs. (1) and (2), the concentrations of the free proteins  $c_{FcRn}$  and  $c_{Fc}$ , and the baseline offset  $\delta$  were treated as floating parameters local to each data set, whereas the association constants  $K_{A(1:1)}$  and  $K_{A(2:1)}$  were optimized as global parameters. The buoyant molar masses were predetermined in separate experiments (see below). Least-squares modeling was performed with the commercial software MLAB (Civilized Software, Bethesda, MD). The statistical analysis of the precision of the derived parameters was based on the standard method of projections of the sum-of-squares surface in parameter

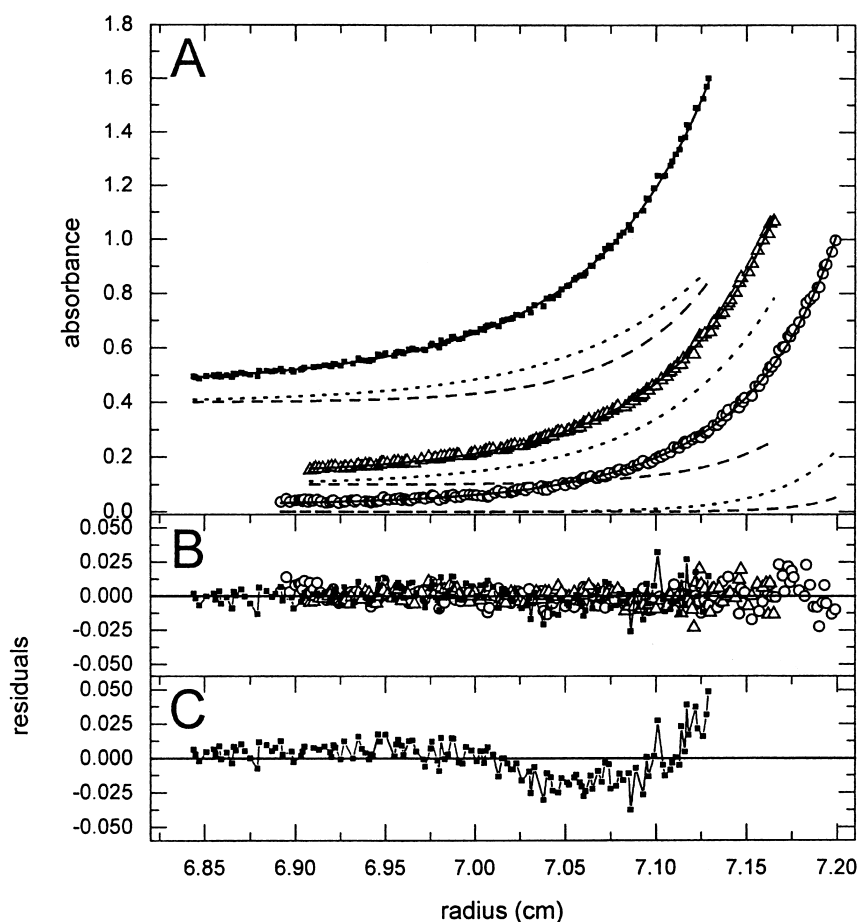


Fig. 2. Sedimentation equilibrium analysis of FcRn interaction with Fc fragment. A: Experimental absorbance profiles of FcRn-Fc mixtures at total concentrations of  $0.56 \mu\text{M}$  FcRn and  $0.47 \mu\text{M}$  Fc at 18,000 rpm, scanned at 230 nm (circles),  $1.95 \mu\text{M}$  FcRn and  $1.35 \mu\text{M}$  Fc at 13,000 rpm, scanned at 280 nm (triangles) (for clarity, data are shown with an offset of 0.1 OD), and  $5.5 \mu\text{M}$  FcRn and  $2.8 \mu\text{M}$  Fc at 12,000 rpm, scanned at 250 nm (squares) (offset by 0.4 OD). Global analysis led to best-fit distributions as indicated by the solid lines, with  $K_{A(1:1)}$  for 1:1 complex formation of  $6.5 \times 10^8 \text{ M}^{-1}$  and an affinity  $K_{A(2:1)}$  for the addition of a second FcRn molecule (formation of 2:1 complex) of  $1.64 \times 10^5 \text{ M}^{-1}$ . The theoretical distributions are shown with the same offset as the fitted data. To illustrate the contribution of the mixed complexes to the observed absorption profiles at the different loading concentrations, the calculated distribution of the 1:1 complex was indicated by the dotted line and the 2:1 complex by the dashed line. B: Residuals of the fit from A. C: Residuals of the best-fit to the highest concentration data shown in A assuming the absence of 2:1 complex formation.

space combined with *F*-statistics. A detailed description of this method can be found elsewhere (Bevington and Robinson, 1992; Press et al., 1992; Schuck, 1994). In short, in this method the parameter for which the error is to be estimated is constrained to non-optimal values. For each value, all other parameters are optimized. The sums of squares of these constrained fits then give the minimal increase in the variance of the fit that is associated with the non-optimal, constrained parameter value. The ratio of this constrained variance to the overall best-fit variance follows *F*-statistics, and therefore it can be readily transformed into a probability for each value of the constrained parameter (Bevington and Robinson, 1992; Press et al., 1992; Schuck, 1994).

### 3. Results

#### 3.1. Behaviour of FcRn, Fc and IgG1 in the centrifugal field and determination of their buoyant molar masses

We first examined the proteins FcRn, Fc and IgG1 individually in the analytical ultracentrifuge over a wide concentration range in order to measure their buoyant molar mass, and to establish the absence of thermodynamic nonidealities, the purity of the samples and the absence of reversible self-association. Fig. 1 shows typical individual concentration profiles of FcRn, Fc and IgG1 in sedimentation equilibrium.

The FcRn data are well described by modeling with an ideal non-interacting component  $A_{\text{FcRn}}(r)$  as given

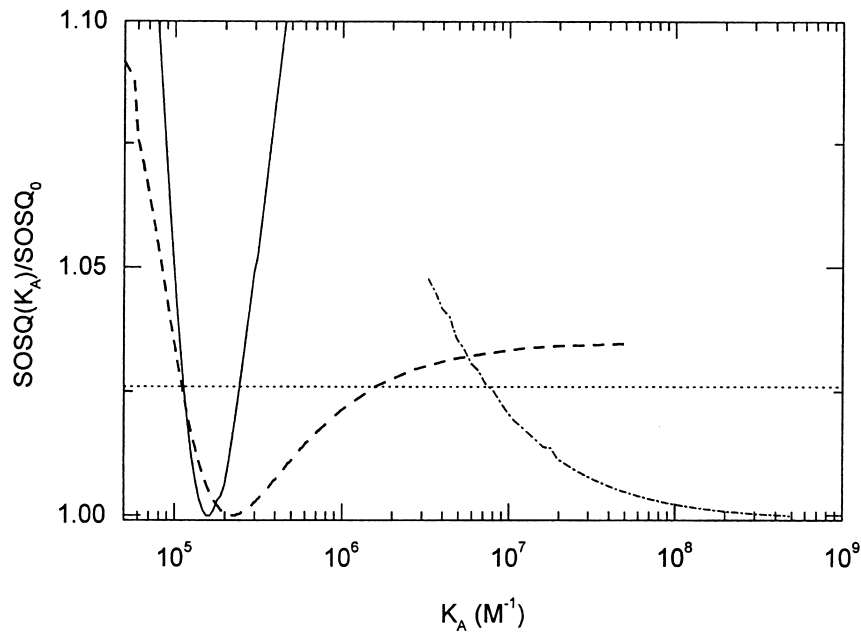


Fig. 3. Projections of the error surface of the global sedimentation equilibrium analyses for the association constant of the 1:1 FcRn-Fc complex formation (dash-dotted line), the 2:1 FcRn-Fc complex formation (solid line) and the 2:1 FcRn-IgG complex formation (dashed line) (Bevington and Robinson, 1992; Press et al., 1992). These curves show the relative increase in the sum of the squared residuals (SOSQ) of the global fit obtained when constraining the parameter value of  $K_A$  to a non-optimal value whilst optimizing all other parameters at each point of the curve. Their minimum values show the best-fit solution for the binding constants, whilst their shapes visualize the information content of the data on the binding constants. The horizontal dotted line indicates the level of increase in the SOSQ that corresponds to the probability of one standard deviation according to  $F$ -statistics ( $n > 1200$ ). Its intersection with the SOSQ curves indicates the uncertainty of the derived optimal parameter values.

in Eq. (2), with buoyant molar mass  $M_{\text{FcRn}}^*$  of 13,500 Da (Fig. 1). This value is consistent with the value obtained from interference optical ultracentrifugation studies with enhanced signal-to-noise ratio (Schuck, 1999). No indications of significant dimerization of FcRn was found in the concentration range studied (although a weak dimerization with an equilibrium dissociation constant above 100  $\mu\text{M}$  cannot be excluded). At higher FcRn concentrations, a slight tendency of aggregation was occasionally observed if the sample was exposed to temperatures above 4°C for a prolonged time. However, this effect was poorly reproducible and could be avoided by using a pre-chilled rotor and carrying out the centrifugation experiments at 4°C.

The analysis of the sedimentation profile obtained from Fc alone was also well-described by the theoretical concentration distribution of an ideal monomeric species in the centrifugal field, following the expression  $A_{\text{Fc}}(r)$  of Eq. (2), with a best-fit buoyant molar mass  $M_{\text{Fc}}^*$  of 14,540 Da (Fig. 1). Similarly, the sedimentation equilibrium distributions of the IgG1 were well-described over a wide concentration range by the analogous single species model with a buoyant molar mass of 40,660 Da, consistent with the value derived elsewhere (Schuck, 1999).

With the buoyant molar masses of the proteins and

their ideal sedimentation behavior established, it can be predicted that the concentration distributions of the 1:1 and 2:1 FcRn:Fc complexes formed reversibly in the ultracentrifuge will follow the expressions  $A_{1:1}(r)$  and  $A_{2:1}(r)$  of Eq. (2). The buoyant molar masses to be expected for the 1:1 and 2:1 complexes are 28,040 and 41,540 Da for the FcRn:Fc complexes, and 54,160 Da and 67,660 Da for the FcRn:IgG1 complexes.

### 3.2. Interaction of FcRn with Fc

For the study of the FcRn interaction with Fc, sedimentation equilibrium experiments were performed at different loading concentrations, molar ratios and rotor speeds. Complex formation was evident by the weight-average buoyant molar mass of the mixture being larger than that of the individual proteins even at very low protein concentrations. This indicates the presence of a high affinity interaction. For the experiments at low and medium protein concentrations, the obtained sedimentation profile can be modeled with one high affinity 1:1 interaction alone (i.e. by Eq. (1) without the term  $A_{2:1}(r)$ , data not shown). However, at higher protein concentrations and higher FcRn to Fc ratio, the data could not be modeled if only 1:1 complex formation (Fig. 2C) was assumed. This clearly indicates the presence of larger FcRn:Fc complexes.

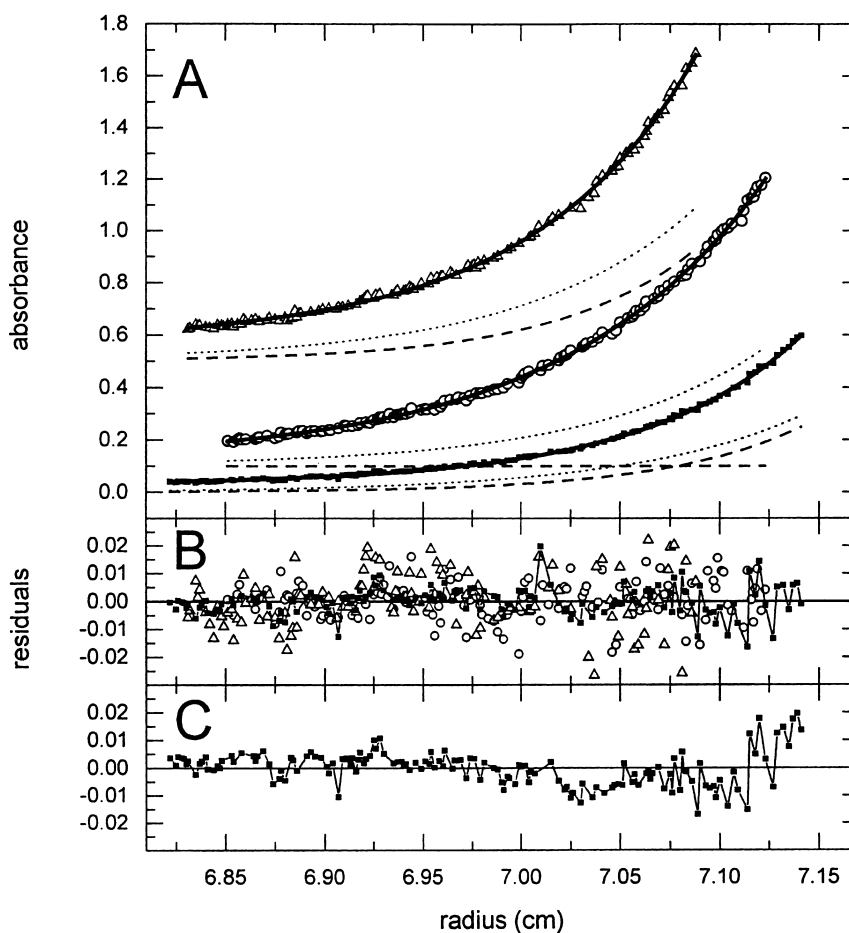


Fig. 4. Sedimentation equilibrium analysis of FcRn interaction with IgG. A: Experimental absorbance profiles of FcRn-IgG mixtures at total concentrations of 1.3  $\mu\text{M}$  FcRn and 4.8  $\mu\text{M}$  IgG, scanned at 250 nm (circles) (shown with an offset of 0.1 OD) and 7.2  $\mu\text{M}$  FcRn and 4.0  $\mu\text{M}$  IgG, scanned at 250 nm (triangles) (offset by 0.5 OD) and scanned at 306 nm (squares). Rotor speed was 8000 rpm. Global best-fit distributions (solid lines) with  $K_A^{(1:1)}$  for 1:1 complex formation of  $6.5 \times 10^8 \text{ M}^{-1}$  (dotted lines) and a 2:1 complex with an affinity of  $K_A^{(2:1)} = 2.17 \times 10^5 \text{ M}^{-1}$  for the addition of a second FcRn molecule (dashed lines). B: Residuals of the fit shown in A. C: Residuals of the best-fit to the highest concentration data shown in A assuming the absence of 2:1 complex formation.

Fig. 2 shows representative data of mixtures of FcRn and Fc in sedimentation equilibrium at different loading concentrations. The global analysis using the model with reversible 1:1 and 2:1 FcRn:Fc complexes according to Eq. (1) led to evenly distributed residuals in the range of the noise of the data acquisition (Fig. 2A and B). Included in Fig. 2A are the calculated distributions of the 1:1 complex (dotted line) and the 2:1 complex (dashed line), demonstrating that the low-affinity 2:1 complex is significantly populated only at higher protein concentrations. A well-known technical difficulty in measuring the binding constants by analytical ultracentrifugation is that for reactants of similar buoyant molar mass, such as  $M_{\text{FcRn}}^*$  and  $M_{\text{Fc}}^*$ , only a lower limit of the association constant can be determined (because the free species cannot be distinguished on the basis of their sedimentation profiles). In the present case, a lower limit of  $7.7 \times 10^6 \text{ M}^{-1}$  for the macroscopic association constant could be established.

A statistical analysis reveals that all values of  $K_{A(1:1)}$  above this limit ( $K_D < 130 \text{ nM}$ ) provide fits of high quality that cannot be statistically discriminated (Fig. 3), while values smaller than  $7.7 \times 10^6 \text{ M}^{-1}$  did not describe the data well. This demonstrates a high affinity of FcRn for Fc to form a 1:1 complex with an affinity that is consistent with previous surface plasmon resonance experiments (Popov et al., 1996). Assuming the presence of two equivalent sites on the Fc for the first FcRn molecule that binds, this corresponds to a free energy of binding of  $> 8.3 \text{ kcal/Mol}$ . However, if these sites are non-equivalent prior to FcRn binding i.e. the IgG1 molecule is asymmetric in the absence of interaction with FcRn, the free energy of binding is 8.7 kcal/Mol.

For the macroscopic binding constant  $K_{A(2:1)}$  for formation of a 2:1 FcRn:Fc complex, a value of  $1.6 \times 10^5 \text{ M}^{-1}$  could be obtained ( $K_D = 6.1 \mu\text{M}$ ). The statistical analysis of the confidence of the derived

binding constants from the global fit to all experimental data sets with mixtures of FcRn and Fc is shown in Fig. 3. The well-defined minimum of the global sum-of-squares profile obtained when constraining  $K_{A(2:1)}$  to different values while optimizing all other parameters, shown by the solid line in Fig. 3, indicates the high information content of the data for the 2:1 complex and the significant contribution of these complexes to the observed sedimentation profiles. This also led to a small error estimate, as calculated by the intersection with the horizontal line in Fig. 3 (which describes the sum-of-squares cut-off value at a confidence level of one standard deviation (Bevington and Robinson, 1992; Press et al., 1992)). The estimated free energy of binding was  $7.0 \pm 0.2$  kcal/Mol for the addition of a second FcRn molecule to a preformed 1:1 complex (assuming the presence of two equivalent orientations of the 1:1 complex). The difference in the free energy of binding of 1.3 kcal/Mol for the second FcRn compared with the first FcRn molecule corresponds to a more than 50 fold difference in the macroscopic binding constants (or more than a 10 fold difference in the microscopic constants) and is statistically highly significant.

### 3.3. Interaction of FcRn with IgG1

In a similar approach, the interaction of FcRn with the complete IgG1 molecule was studied by global sedimentation equilibrium analysis of several data sets obtained under a variety of conditions (Fig. 4). In the study of this interaction, the technical difficulty of ultracentrifugation to distinguish species of close buoyant molar masses in mixtures limits the resolution of the higher molar mass components. Due to the smaller relative differences in the buoyant molar masses of the 1:1 and 2:1 complexes of FcRn with IgG1 as compared with the complexes with Fc (see above), smaller differences in the quality of fits by models with and without a 2:1 complex can be expected.

Nevertheless, in the analysis of the experimental absorbance profiles both the formation of 1:1 complexes as well as complexes larger than 1:1 was apparent. First, we performed experiments of a FcRn-IgG1 mixture at high concentration and 2:1 molar ratio in order to achieve a high population of the larger complexes. Here, only a relatively poor fit can be obtained if using a model lacking higher order complexes (Fig. 4C), although the data are not as clear as for the Fc interaction (Fig. 2C). Second, we analyzed simultaneously the experimental absorbance profiles obtained in experiments both with lower molar ratios and at lower protein concentrations. A good fit could be achieved with the model of Eqs. (1) and (2), including the term for the 2:1 complex (Fig. 4A and B) with a best-fit estimate for  $K_{A(2:1)}$  of  $2.17 \times 10^5$

$M^{-1}$  ( $K_D = 4.6 \mu M$ ). The statistical analysis of the information content of the data shown in Fig. 3 (dashed line) describes a relatively steep increase in the variance of the fit at lower, sub-optimal values of  $K_{A(2:1)}$ . This demonstrates the significance of the 2:1 complex in the global analysis.

Unfortunately, a significant correlation in the determination of the two binding constants  $K_{A(1:1)}$  and  $K_{A(2:1)}$  was observed. If a higher confidence limit would be applied in the statistical data analysis of Fig. 3, stronger 2:1 complex formation could not be excluded. The calculated free energy of binding for the second FcRn molecule was 7.1 (6.8–8.2) kcal/Mol. It can be concluded that within the error limits of the centrifugation experiments, the obtained binding constants of FcRn for the interaction with IgG1 and Fc fragment are identical.

## 4. Discussion

In the current study the affinity of interaction of a soluble form of mouse FcRn for mouse Fc or IgG1 has been analyzed using sedimentation equilibrium analyses. For both ligands, the data clearly show the existence of a high and low affinity interaction site for FcRn. The nature of the interaction of IgG1 and IgG1-derived Fc with FcRn are the same within the bounds of experimental error. This is consistent with both in vitro and in vivo data demonstrating that mouse Fc fragments and IgG molecules are functionally equivalent (Kim et al., 1994a; Popov et al., 1996). The data fit a model in which a high affinity 1:1 FcRn:Fc/IgG complex is first formed, and subsequently a second FcRn molecule binds with lower affinity. Whether this asymmetric interaction is general for other IgG isotypes/species requires further investigation since in the current study only the interaction of mouse IgG1 (or Fc) with insect cell expressed FcRn has been analyzed.

The observations for the mouse FcRn:IgG/Fc interaction provide an explanation for the apparent discrepancies that were reported for the stoichiometry of this interaction (Popov et al., 1996) and in vivo analysis of a recombinant Fc-hybrid fragment suggesting that two FcRn interaction sites per IgG/Fc were needed for FcRn-mediated activity (Kim et al., 1994b). Under the conditions of the in vitro stoichiometry experiments (Popov et al., 1996) only the high affinity site for FcRn binding on IgG/Fc would be occupied. A determination of whether the differing classes of binding sites are due to flexibility of the IgG or Fc molecule that results in distortion of the second site following occupation of the first high affinity site, or to steric blockade of the second site (or a combination of both) requires further experimentation. In this con-

text, recent modeling studies have indicated that the CH2 domain of Fc reorientates following FcRn binding, which would in turn interfere with optimal binding of FcRn to the second interaction site (Weng et al., 1998). This model would argue for the induction of the two classes of distinct FcRn interaction sites following the initial interaction of FcRn with one site on IgG/Fc. Consistent with this, the IgG molecule is known to be flexible at the CH2–CH3 domain interface and displays segmental motion in solution (Nezlin, 1990; Zheng et al., 1992). The data for the interaction of IgG or Fc with FcRn are reminiscent of those reported for the IgE(Fc):FcR $\epsilon$ 1 receptor interaction, where 1:1 complexes were observed despite the presence of two possible interaction sites (Keown et al., 1995; Robertson, 1993). Fluorescence resonance energy transfer measurements support the existence of a bent configuration of mouse IgE in solution, with IgE being less flexible than human IgG1 (Zheng et al., 1992). In addition, the IgE:FcR $\epsilon$ 1 interaction represents a situation where the asymmetry is so extreme that the second site is not occupied during sedimentation equilibrium centrifugation (Keown et al., 1995).

In contrast to our earlier *in vitro* stoichiometry studies indicating a 1:1 interaction for mouse FcRn with mouse IgG1/Fc (Popov et al., 1996), in other gel filtration and calorimetry experiments a 2:1 stoichiometry for rat FcRn:Fc complexes was reported (Huber et al., 1993). In addition, in the latter study the calorimetry data supported an interaction model of a 'single class of non-interacting binding site(s)' (Huber et al., 1993). This suggests that there may be species differences or, as suggested earlier (Popov et al., 1996) differences due to the expression systems used for the production of recombinant FcRn. In this respect, the insect cell expressed mouse FcRn in the current study has high mannose type carbohydrate, whereas rat FcRn expressed in CHO cells has complex N-linked glycosylation (Vaughn and Bjorkman, 1998). Precedence in another system for the existence of functional differences that are dependent on the expression host comes from the analysis of activity in binding to C1q and Fc $\gamma$ RI of chimeric human-mouse IgGs with altered (CH2-domain associated) carbohydrate structure (Tsuchiya et al., 1989; Wright and Morrison, 1994). Furthermore, the IgG associated carbohydrate does not play a direct role in contacting C1q or Fc $\gamma$ RI, indicating that longer range effects of carbohydrate are possible. Therefore, similar long range effects may play a role in the interaction of different glycoforms of FcRn with cognate ligands.

The apparent asymmetry of the mouse FcRn interaction sites on IgG or Fc, with macroscopic affinities differing by about 50 fold, raises the question as to how relevant this is to the physiological situation where FcRn is membrane bound. It is plausible that

the occupancy of the lower affinity site may be high *in vivo* due to dimerization of FcRn mediated through interactions in its transmembrane and cytoplasmic tail. This dimer formation might occur following initial binding of FcRn to the high affinity site on IgG. It is tempting to speculate that such ligand-induced dimerization could play a role in the trafficking of FcRn, for which the molecular details are currently unknown. In support of this, evidence for the existence of FcRn dimers *in vivo* has been obtained using electron irradiation (Simister and Rees, 1985). In addition, the existence of a different type of FcRn dimer, in which association occurs predominantly through  $\alpha$ 3 domain and  $\beta$ 2-microglobulin residues (i.e. an FcRn-FcRn dimer), is supported by surface plasmon resonance analyses (Raghavan et al., 1995b; Vaughn and Bjorkman, 1997) and structural studies (Burmeister et al., 1994) using rat FcRn. FcRn associated carbohydrate has been shown to play a role in this second mode of dimerization (Vaughn and Bjorkman, 1998), and this dimer has been reported to have a higher affinity for IgG binding than monomeric FcRn (Raghavan et al., 1995b; Vaughn and Bjorkman, 1997). The two types of FcRn dimers have been suggested to form networks of 'oligomeric ribbons' (reviewed in Raghavan and Bjorkman, 1996), but direct evidence for the existence of these oligomers *in vivo* has for obvious technical reasons not been obtained. In the current study evidence for the existence of FcRn dimers which have high affinity for Fc or IgG was not found, but this may again be due to differences in the expression hosts and/or IgG/FcRn species used. In this respect, it has been reported that CHO cell expressed, mouse FcRn forms 2:1 FcRn:Fc complexes, which have been suggested to be due to the formation of FcRn dimer:Fc complexes in which FcRn:FcRn dimerization is stabilized by a 'carbohydrate handshake' between sugars on the  $\alpha$ 3 domains (Vaughn and Bjorkman, 1998).

The current study further extends our knowledge concerning the mouse FcRn:IgG/Fc interaction using insect cell expressed FcRn and native, myeloma expressed IgG1 or IgG1-derived Fc. Quantitative data for the affinities of the two classes of binding site in an asymmetric FcRn:IgG:FcRn (or FcRn:Fc:FcRn) interaction have been obtained. This study has relevance to gaining a better understanding of the relationship between *in vitro* binding studies and how FcRn trafficks *in vivo*, in addition to suggesting further experiments to investigate the functional asymmetry of the IgG molecule.

#### Acknowledgements

We are indebted to Dr Victor Ghetie for providing

the mouse IgG1 and Fc fragments used in this study. This work was supported by the NIH (Grant number RO1 AI39167) and Robert Welch Foundation (Grant number I-1333).

## References

- Bevington, P.R., Robinson, D.K., 1992. Data Reduction and Error Analysis for the Physical Sciences. McGraw-Hill, New York.
- Burmeister, W.P., Huber, A.H., Bjorkman, P.J., 1994. Crystal structure of the complex of rat neonatal Fc receptor with Fc. *Nature* 372, 379–383.
- Ghetie, V., Hubbard, J.G., Kim, J.K., Tsen, M.F., Lee, Y., Ward, E.S., 1996. Abnormally short serum half-lives of IgG in  $\beta$ 2-microglobulin-deficient mice. *Eur. J. Immunol.* 26, 690–696.
- Ghetie, V., Ward, E.S., 1997. FcRn: the MHC class I-related receptor that is more than an IgG transporter. *Immunol. Today* 18, 592–598.
- Huber, A.H., Kelley, R.F., Gastinel, L.N., Bjorkman, P.J., 1993. Crystallization and stoichiometry of binding of a complex between a rat intestinal Fc receptor and Fc. *J. Mol. Biol.* 230, 1077–1083.
- Israel, E.J., Patel, V.K., Taylor, S.F., Marshak-Rothstein, A., Simister, N.E., 1995. Requirement for a  $\beta$ 2-microglobulin-associated Fc receptor for acquisition of maternal IgG by fetal and neonatal mice. *J. Immunol.* 154, 6246–6251.
- Israel, E.J., Wilsker, D.F., Hayes, K.C., Schoenfeld, D., Simister, N.E., 1996. Increased clearance of IgG in mice that lack  $\beta$ 2-microglobulin: possible protective role of FcRn. *Immunology* 89, 573–578.
- Junghans, R.P., Anderson, C.L., 1996. The protection receptor for IgG catabolism is the  $\beta$ 2-microglobulin-containing neonatal intestinal transport receptor. *Proc. Natl. Acad. Sci. USA* 93, 5512–5516.
- Junghans, R.P., 1997. Finally! The Brambell receptor (FcRB). Mediator of transmission of immunity and protection from catabolism for IgG. *Immunol. Res.* 16, 29–57.
- Kim, J.K., Tsen, M.F., Ghetie, V., Ward, E.S., 1994a. Localization of the site of the murine IgG1 molecule that is involved in binding to the murine intestinal Fc receptor. *Eur. J. Immunol.* 24, 2429–2434.
- Kim, J.K., Tsen, M.F., Ghetie, V., Ward, E.S., 1994b. Catabolism of the murine IgG1 molecule: evidence that both CH2-CH3 domain interfaces are required for persistence of IgG1 in the circulation of mice. *Scand. J. Immunol.* 40, 457–465.
- Keown, M.B., Ghirlando, R., Young, R.J., Beavil, A.J., Owens, R.J., Perkins, S.J., Sutton, B.J., Gould, H.J., 1995. Hydrodynamic studies of a complex between the Fc fragment of human IgE and a soluble fragment of the Fc $\epsilon$ RI  $\alpha$  chain. *Proc. Natl. Acad. Sci. USA* 92, 1841–1845.
- Laue, T.M., Shah, B.D., Ridgeway, T.M., Pelletier, S.L., 1992. Computer-aided interpretation of analytical sedimentation data for proteins. In: Harding, S.E., Rowe, A.J., Horton, J.C. (Eds.), *Analytical Ultracentrifugation in Biochemistry and Polymer Science*. The Royal Society of Chemistry, Cambridge, pp. 90–125.
- Medesan, C., Matesoi, D., Radu, C., Ghetie, V., Ward, E.S., 1997. Delineation of the amino acid residues involved in transcytosis and catabolism of mouse IgG1. *J. Immunol.* 158, 2211–2217.
- Nezlin, R., 1990. Internal movements of immunoglobulin molecules. *Adv. Immunol.* 48, 1–40.
- Popov, S., Hubbard, J.G., Kim, J., Ober, B., Ghetie, V., Ward, E.S., 1996. The stoichiometry and affinity of the interaction of murine Fc fragments with the MHC class I-related receptor, FcRn. *Mol. Immunol.* 33, 521–530.
- Press, W.H., Teukolsky, S.A., Vetterling, W.T., Flannery, B.P., 1992. *Numerical Recipes in C*. Cambridge University Press, Cambridge.
- Raghavan, M., Chen, M.Y., Gastinel, L.N., Bjorkman, P.J., 1994. Investigation of the interaction between the class I MHC-related Fc receptor and its immunoglobulin G ligand. *Immunity* 1, 303–315.
- Raghavan, M., Bonagura, V.R., Morrison, S.L., Bjorkman, P.J., 1995a. Analysis of the pH dependence of the neonatal Fc receptor/immunoglobulin G interaction using antibody and receptor variants. *Biochemistry* 34, 14649–14657.
- Raghavan, M., Wang, Y., Bjorkman, P.J., 1995b. Effects of receptor dimerization on the interaction between the class I major histocompatibility complex-related Fc receptor and IgG. *Proc. Natl. Acad. Sci. USA* 92, 11200–11204.
- Raghavan, M., Bjorkman, P.J., 1996. Fc receptors and their interactions with immunoglobulins. *Annu. Rev. Cell Dev. Biol.* 12, 181–220.
- Rivas, G.W., Stafford, W., Minton, A.P., 1999. *Methods: A Companion to Methods in Enzymology*. In press.
- Roberts, D.M., Guenther, M., Rodewald, R., 1990. Isolation and characterization of the Fc receptor from the fetal yolk sac of the rat. *J. Cell Biol.* 111, 1867–1876.
- Robertson, M.W., 1993. Phage and *Escherichia coli* expression of the human high affinity immunoglobulin E receptor alpha-subunit ectodomain. Domain localization of the IgE-binding site. *J. Biol. Chem.* 268, 12736–12743.
- Rodewald, R., Lewis, D.M., Kraehenbuhl, J.P., 1983. Immunoglobulin G receptors of intestinal brush borders from neonatal rats. *Ciba Found. Symp.* 95, 287–299.
- Rodewald, R., Kraehenbuhl, J.P., 1984. Receptor-mediated transport of IgG. *J. Cell Biol.* 99, 159s–164s.
- Schuck, P., 1994. Simultaneous radial and wavelength analysis in the analytical ultracentrifuge. *Progress in Colloid and Polymer Science* 94, 1–13.
- Schuck, P., 1999. Sedimentation equilibrium analysis of interference optical data by systematic noise decomposition. *Anal. Biochem.* 272, 199–208.
- Simister, N.E., Mostov, K.E., 1989. An Fc receptor structurally related to MHC class I antigens. *Nature* 337, 184–187.
- Simister, N.E., Rees, A.R., 1985. Isolation and characterization of an Fc receptor from neonatal rat small intestine. *Eur. J. Immunol.* 15, 733–738.
- Tschiya, N., Endo, T., Matsuta, K., Yoshinoya, S., Aikawa, T., Kosuge, E., Takeuchi, F., Miyamoto, T., Kobata, A., 1989. Effects of galactose depletion from oligosaccharide chains on immunological activities of human IgG. *J. Rheumatol.* 16, 285–290.
- Vaughn, D.E., Bjorkman, P.J., 1997. High-affinity binding of the neonatal Fc receptor to its IgG ligand requires receptor immobilization. *Biochemistry* 36, 9374–9380.
- Vaughn, D.E., Bjorkman, P.J., 1998. Structural basis of pH-dependent antibody binding by the neonatal Fc receptor. *Structure* 6, 63–73.
- Weng, Z., Gulukota, K., Vaughn, D.E., Bjorkman, P.J., DeLisi, C., 1998. Computational determination of the structure of rat Fc bound to the neonatal Fc receptor. *J. Mol. Biol.* 282, 217–225.
- Wright, A., Morrison, S.L., 1994. Effect of altered CH2-associated carbohydrate structure on the functional properties and in vivo fate of chimeric mouse-human immunoglobulin G1. *J. Exp. Med.* 180, 1087–1096.
- Zheng, Y., Shopes, R., Holowka, D., Baird, B., 1992. Dynamic conformations compared for IgE and IgG1 in solution and bound to receptors. *Biochemistry* 31, 7446–7456.